

## Voltage-dependent Conductance Changes in a Nonvoltage-activated Sodium Current from a Mast Cell Line

A.B. Parekh

Department of Physiology, University of Oxford, Parks Road, Oxford OX1 3PT, UK

Received: 12 March 1998/Revised: 5 June 1998

**Abstract.** Nonexcitable cells do not express voltage-activated  $\text{Na}^+$  channels. Instead, selective  $\text{Na}^+$  influx is accomplished through GTP-activated  $\text{Na}^+$  channels, the best characterized of which are found in renal epithelia. We have described recently a GTP-dependent  $\text{Na}^+$  current in rat basophilic leukemia (RBL) cells that differs from previous reported  $\text{Na}^+$  channels in several ways including selectivity, pharmacology and mechanism of activation. In this report, we have investigated the biophysical properties of the RBL cell  $\text{Na}^+$  current using the whole cell patch-clamp technique. Following activation by 250–500  $\mu\text{M}$  GTP $\gamma\text{S}$ , hyperpolarizing steps to a fixed potential (–100 mV) from a holding potential of 0 mV evoked transient inward  $\text{Na}^+$  currents that declined during the pulse. If the holding potential was made more positive (range 0 to +100 mV), then the amplitude of the transient inward current evoked by the hyperpolarization increased steeply, demonstrating that the conductance of the channels was voltage-dependent. Using a paired pulse protocol (500 msec pulses to –100 mV from a holding potential of 0 mV), it was found that the peak amplitude of the current during the second pulse became larger as the interpulse potential became more positive. In addition, increasing the time at which the cells were held at positive potentials also resulted in larger currents, indicating a time-dependent conductance change. With symmetrical  $\text{Na}^+$  solutions, outward currents were recorded at positive potentials and these demonstrated both a time- and voltage-dependent increase in conductance. The results show that a nonvoltage activated  $\text{Na}^+$  channel in an electrically nonexcitable cell undergoes prominent

voltage-dependent transitions. Possible mechanisms underlying this voltage dependency are discussed.

**Key words:** Sodium current — Voltage-dependent — Conductance

### Introduction

Although  $\text{Ca}^{2+}$  is the main cation used in intracellular signaling, changes in the cytoplasmic free  $\text{Na}^+$  concentration can regulate several cellular processes. Increases in intracellular  $\text{Na}^+$  levels have been implicated in cell volume regulation (Kaplan, Mount & Delpire, 1996) and modulation of excitability through changes in activities both of ion carriers ( $\text{Na}^+/\text{Ca}^{2+}$  exchange and  $\text{Na}^+/\text{K}^+$  ATPases, Hancox & Levi, 1995) as well as channels (e.g.,  $\text{Na}^+$ -activated  $\text{K}^+$  channels in heart, Kameyama, et al., 1984). Activation of cell-surface mitogen receptors in lymphocytes or vasopressin receptors in fibroblasts have been found to elevate intracellular  $\text{Na}^+$  concentration by twofold (Harootunian et al., 1989), and this might contribute to the overall response. In platelets, changes in intracellular  $\text{Na}^+$  have been reported to alter the affinity of  $\alpha_2$ -adrenergic receptor for adrenaline (Motulsky & Insel, 1983).

Because cells do not appear to store  $\text{Na}^+$  within intracellular compartments, the major mechanism for evoking an increase in intracellular  $\text{Na}^+$  concentration is via  $\text{Na}^+$  influx into the cell. In excitable cells, this is accomplished largely through  $\text{Na}^+$ -selective voltage-gated channels (Hille, 1992), although nonselective channels with a finite permeability to  $\text{Na}^+$  can provide an alternative entry pathway. The latter include both  $\text{Ca}^{2+}$ -activated nonselective channels as well as ligand-gated ones (Hille, 1992). In nonexcitable cells, voltage-gated  $\text{Na}^+$  channels are rather rare and nonselective pathways are more prevalent. In the specialized transporting renal

Correspondence to: A.B. Parekh

**Abbreviations:** GTP $\gamma\text{S}$ , guanosine 5'-3-O-(thio)triphosphate; RBL, Rat Basophilic Leukemia

epithelia, a variety of Na<sup>+</sup>-selective voltage-independent channels have been described (Garty & Benos, 1988; Palmer, 1992). Similar Na<sup>+</sup> channels have been found in macrophages (Negulyaev & Vedernikova, 1994) and A431 carcinoma cells (Negulyaev, Vedernikova & Mozhayeva, 1994). These channels are not activated by changes in the membrane potential, but instead seem to require GTP analogues like GTP $\gamma$ S. The channels are largely voltage-independent, in that changing the membrane potential does not alter the conductance other than through the electrical driving force.

However, the renal epithelial-type Na<sup>+</sup> channel is not the only one found in nonexcitable cells. Recently, we have characterized a Na<sup>+</sup>-selective channel in rat basophilic leukemia (RBL) cells, which differs in its ionic selectivity, pharmacology and mechanism of activation from the Na<sup>+</sup>-selective channels described so far in other nonexcitable cells (Parekh, 1996). Although the RBL cell Na<sup>+</sup> current required GTP $\gamma$ S for activation in patch-clamp experiments and could not be activated simply by depolarizing the membrane potential, the current declined rapidly during hyperpolarizing pulses despite the large sustained electrical gradient for Na<sup>+</sup> entry. In this paper, we have investigated this voltage-dependence further. We find that the conductance of the Na<sup>+</sup> channels is strongly voltage-dependent. Depolarizations can substantially increase the conductance whereas hyperpolarizations reduce it. The voltage-dependent conductance change is also time-dependent. Our results demonstrate that a non-voltage-activated current in an electrically nonexcitable cell can undergo prominent voltage-dependent transitions in conductance.

## Materials and Methods

Rat basophilic leukemia cells (RBL-2H3) cells were kindly supplied by Michael Pilot, Max Planck Institute for Biophysical Chemistry, Goettingen, Germany and were cultured essentially as previously described (Parekh, 1996). Patch-clamp experiments were conducted in the tight-seal whole-cell configuration at room temperature (18–25°C) as previously described (Hamill et al., 1981). Patch pipettes were pulled from borosilicate glass (Hilgenberg), sylgard coated and fire-polished. Pipettes had d.c. resistances of 2.5–4 M $\Omega$  when filled with standard internal solution that contained (in mM): cesium glutamate 145, NaCl 8, MgCl<sub>2</sub> 1, MgATP 1, InsP<sub>3</sub> 0.03, EGTA 10, HEPES 10, GTP $\gamma$ S 0.3, pH 7.2 with CsOH. A correction of +10 mV was applied for the subsequent liquid junction potential. Extracellular solution contained (in mM): NaCl 145, KCl 2.8, CaCl<sub>2</sub> 10, MgCl<sub>2</sub> 2, CsCl 10, glucose 10, HEPES 10, pH 7.2 (NaOH). CsCl was present to block the activity of the inwardly rectifying potassium channel. High resolution current recordings were acquired by a computer-based patch-clamp amplifier system (EPC-9, HEKA Electronics, Germany). Capacitative currents were cancelled before each voltage ramp using the automatic compensation of the EPC-9. Series resistance was between 5 and 15 M $\Omega$ . Currents were filtered using an 8-pole Bessel filter at 2.5 kHz and digitized at 100  $\mu$ sec. The Na<sup>+</sup> current was measured using either voltage ramps (–100 to +100 mV in 50 msec) or voltage steps (pulses to –80 mV for 200 msec) applied every 2 secs using PULSE software (HEKA Electronics)

on a 9500 PowerMac. Cells were held at 0 mV between pulses. All currents were leak subtracted by averaging the first two to four ramps/steps after breaking in and then subtracting this from all subsequent traces. Several parameters (capacitance, series resistance, holding current) were displayed simultaneously on a second monitor at a slower rate (2 Hz) using the X-Chart display (HEKA Electronics). Data are presented as mean  $\pm$  SEM, and statistical evaluation was carried out using Students' unpaired *t*-test.

## Results

### VOLTAGE-DEPENDENCE OF Na<sup>+</sup> CURRENT

Dialysis of individual RBL cells with the nonhydrolyzable GTP analogue, GTP $\gamma$ S, activates a Na<sup>+</sup>-selective current (Parekh, 1996). This current will henceforth be referred to as the GTP-Induced Na<sup>+</sup> Current ( $I_{\text{GINa}}$ ).  $I_{\text{GINa}}$  can be conveniently followed by applying voltage ramps (–100 to +100 mV in 50 msec) every 2 sec from a holding potential of 0 mV, as described in Parekh (1996). Following the onset of whole-cell recording, a latency of between 60–600 sec precedes the activation of  $I_{\text{GINa}}$  (Parekh, 1996). The current then develops slowly, requiring several tens of seconds to reach a steady level. A typical example of this behavior is shown in Fig. 1Ai, where the inward current (normalized to cell capacitance) has been measured from the voltage ramps at –80 mV and is plotted as a function of time after breaking into the cell. One striking property of  $I_{\text{GINa}}$  is that the current exhibits a marked decline in amplitude during step changes in the membrane voltage. From the holding potential of 0 mV, 1-sec hyperpolarizations to voltages  $\leq$  –40 mV result in a steep mono-exponential decline of the current, whereas weaker hyperpolarizations or depolarizations do not evoke such responses (Parekh, 1996 and Fig. 1Aii). The following experiments were aimed at examining this voltage-dependent behaviour of  $I_{\text{GINa}}$  in more detail.

### DEPOLARIZATIONS INCREASE CONDUCTANCE

In Fig. 1B, cells were held initially at 0 mV and then clamped at potentials between –20 and +100 mV for 500 msec (conditioning pulses). The voltage was then stepped to –100 mV (test pulse) for 100 msec before returning back to 0 mV. This protocol is depicted in the upper panel of Fig. 1B. The middle panel shows the small background currents that were generated using this pulse sequence shortly after the onset of whole-cell recording (40–70 sec), when  $I_{\text{GINa}}$  had not activated. The lower panel of Fig. 1B depicts the currents evoked by the same protocol after  $I_{\text{GINa}}$  had developed. As the conditioning pulse becomes more positive, larger instantaneous currents are recorded during the test pulses. The traces marked –20 and +100 mV in Fig. 1B refer to the

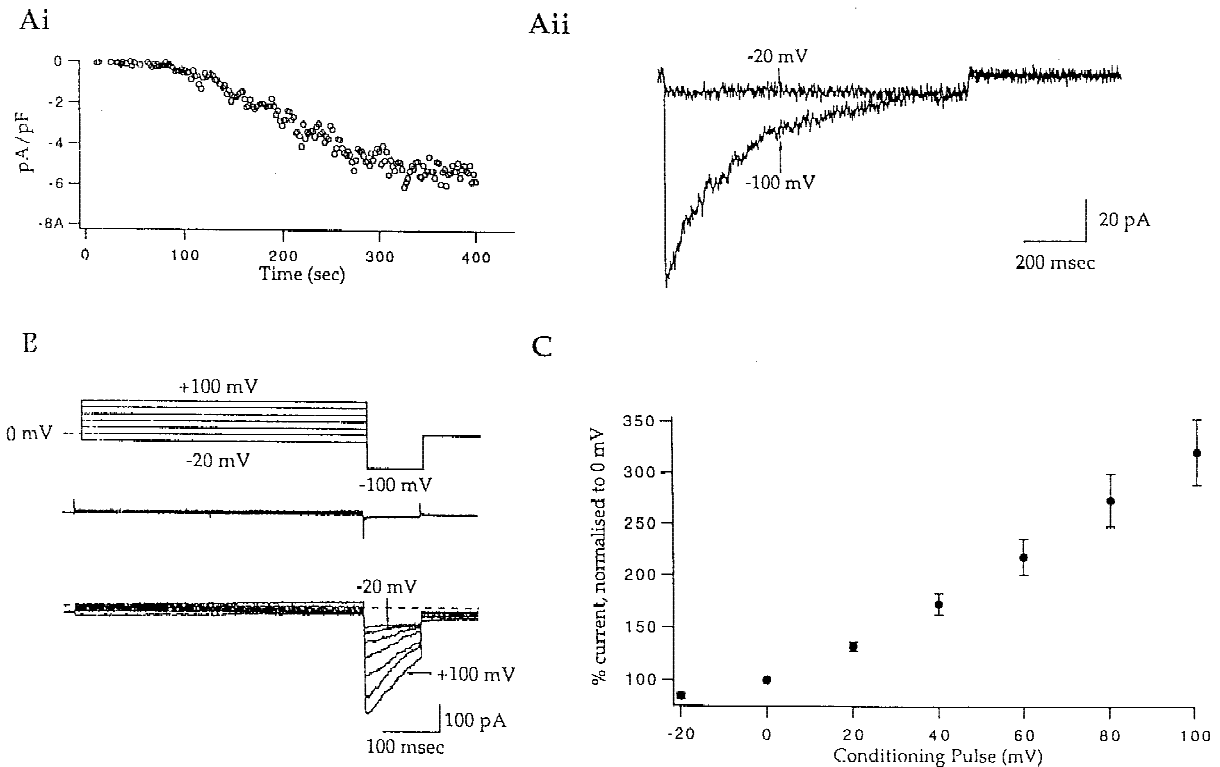


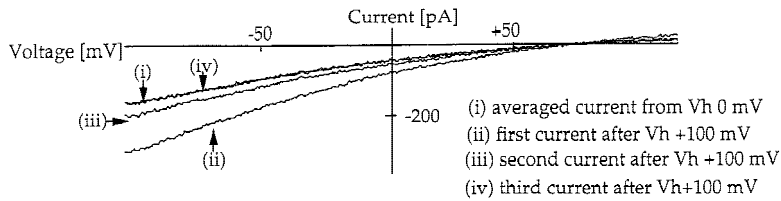
**Fig. 1.** Voltage-dependent gating of  $I_{GINa}$ . (Ai) Development of  $I_{GINa}$  during whole-cell recording. The cells were clamped at 0 mV.  $I_{GINa}$  was monitored by voltage ramps (-100 to +100 mV in 50 msec). The current was measured at -80 mV. (Aii) A large hyperpolarizing step from 0 to -100 mV resulted in decay of the current whereas a smaller pulse to -20 mV did not. (B) Increasing the size of depolarizing pulses (conditioning pulses in text) increased the instantaneous peak current on pulsing to -100 mV. The upper current recordings are the background currents obtained using the voltage protocol (top panel) shortly after break-in. At this time,  $I_{GINa}$  had not developed. The bottom panel shows the currents using the same voltage protocol after  $I_{GINa}$  had activated. The background traces have been subtracted. Dotted line represents zero current level. In (C) the data from 10 cells have been pooled together. Along the ordinate is plotted % peak current during the -100 mV step. The current obtained on pulsing to -100 mV when the conditioning pulse was 0 mV is taken as 100%. The abscissa is the conditioning pulse voltage i.e., the voltage at which the cell was held before stepping to -100 mV.

respective conditioning pulses. The test pulse was the same (-100 mV) for both cases. The conditioning pulse to +100 mV increased the peak amplitude of the test pulse by more than threefold compared with the conditioning pulse to -20 mV. Pooled data from 10 cells are summarized in Fig. 1C. Increasingly positive conditioning pulses generate monotonically larger  $I_{GINa}$ , measured during the test pulses. Because the electrical driving force for  $Na^+$  ions through  $GINa$  channels during the test pulse is always the same irrespective of the conditioning pulse (Vh- $E_{Na}$  i.e., -100 -70 mV), the larger currents during the test pulses reflect an increased whole cell  $GINa$  conductance that arises during the conditioning pulse. Conditioning pulses that depolarize the membrane potential increase  $Na^+$  conductance whereas hyperpolarizing pulses reduce it.

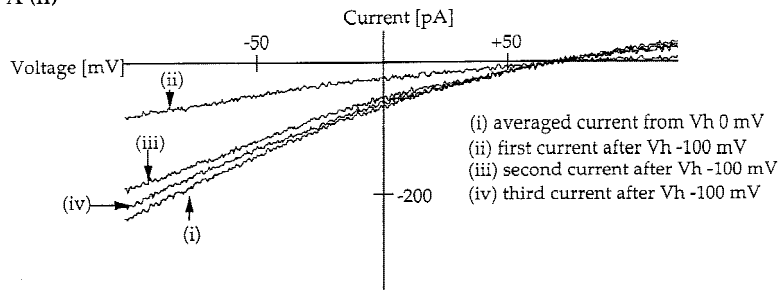
The voltage-dependent changes in whole cell  $GINa$  conductance were examined further using voltage ramps. In these experiments, cells were first held at 0 mV and fast voltage ramps were applied (-100 to +100 mV in 50

msec) to track the development of  $I_{GINa}$ . The holding potential was then changed to different voltages (range -100 to +100 mV in 20-mV increments) and the cells were held at each voltage for 10 sec. No ramps were given during this time. Thereafter, the potential was returned to 0 mV and the fast ramps were then resumed. The effects of changing the holding potential on these subsequent ramp currents are shown in Fig. 2 for two different voltages (-100 and +100 mV). For the positive holding potential (Fig. 2A(i)), the first ramp current after holding at +100 mV for 10 sec was increased, and then the currents declined quickly to reach a level similar to that at a holding potential of 0 mV. This was achieved by the third or fourth ramp (i.e., 6-8 sec). For the hyperpolarizing holding potential on the other hand (Fig. 2A(ii)), the first ramp current was reduced but then subsequent currents grew such that after around 8 seconds the ramp currents were similar to the preceding ones obtained from a holding potential of 0 mV. The graph of Fig. 2B depicts the size of the first ramp current (measured at

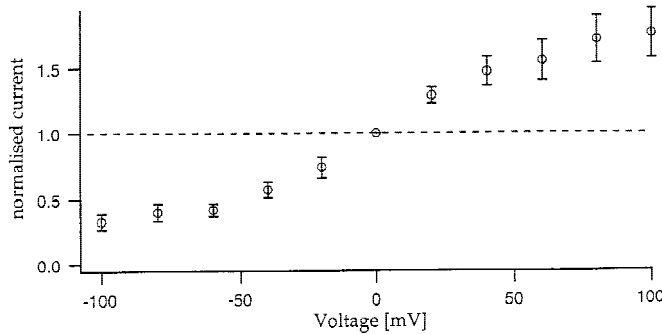
A (i)



A (ii)



B



-80 mV) following a 10-sec voltage clamp at the different holding potentials from 4 cells. Depolarization above 0 mV increase the amplitude of the subsequent voltage ramp-evoked current whereas hyperpolarizations reduced it, consistent with the notion of voltage-dependent changes in sodium channel conductance.

#### TIME-DEPENDENT CONDUCTANCE INCREASE

To examine the time course of the voltage-dependent increase in whole cell  $\text{Na}^+$  channel conductance, cells were held at 0 mV and then the potential was stepped to -100 mV for 200 msec. The cells were then held at a series of different interpulse potentials (20–100 mV) for varying times (20, 40, 80, 160, 320, 640, 1280 msec) before being clamped again at -100 mV. Figure 3A shows the time-dependent recovery of the  $\text{Na}^+$  conductance at three different voltages: 0, +40 and +80 mV. For clarity, the currents evoked after step pulses to -100 mV after 20 msec have been omitted. At 0 mV, full recovery

**Fig. 2.** Voltage-dependent changes in conductance of  $I_{\text{GINa}}$  using ramps. Following the development of  $I_{\text{GINa}}$  (tracked by applying the voltage ramps), cells were clamped at different potentials for 10 sec before the ramps were resumed. Following the termination of the 10 sec pulse, the cells were returned to 0 mV for 20 msec before the ramps were started. In A(i), the cell was clamped at +100 mV for 10 sec. Trace (i) represents the average of 5 ramp currents taken immediately prior to clamping the cell at +100 mV. Trace (ii) is the first ramp taken after holding at +100 mV, and traces (iii) and (iv) were taken 2 and 4 sec after trace (i). In A (ii), the same cell was clamped at -100 mV instead. In B, the current measured at -80 mV in the first ramp after the cell was clamped at different potentials (normalized to the current from the ramps taken from the holding potential of 0 mV) is plotted against the clamp potential. Each point is the mean of at least 4 cells.

occurred after more than 1 sec. At +40 mV, recovery time was 306 msec and at +80 mV it was 184 msec. At positive potentials,  $I_{\text{GINa}}$  dramatically increased in amplitude as the interpulse potential time was increased. In fact, the peak currents on stepping to -100 mV the second time after an interpulse of 40 msec or more could be severalfold larger than the peak currents obtained from pulsing to -100 mV for the first pulse. In Fig. 3B, the time at which  $I_{\text{GINa}}$  had recovered to its initial amplitude (i.e., the peak amplitude reached during the first hyperpolarizing step from a holding potential of 0 mV) is plotted against interpulse potential. Each point is the mean of between 3 and 7 cells and demonstrates that recovery is substantially faster at more positive potentials.

#### VOLTAGE- AND TIME-DEPENDENT OUTWARD $\text{Na}^+$ CURRENTS

Because the  $\text{Na}^+$  conductance increases during depolarizing potentials, one might expect that the outward  $\text{Na}^+$

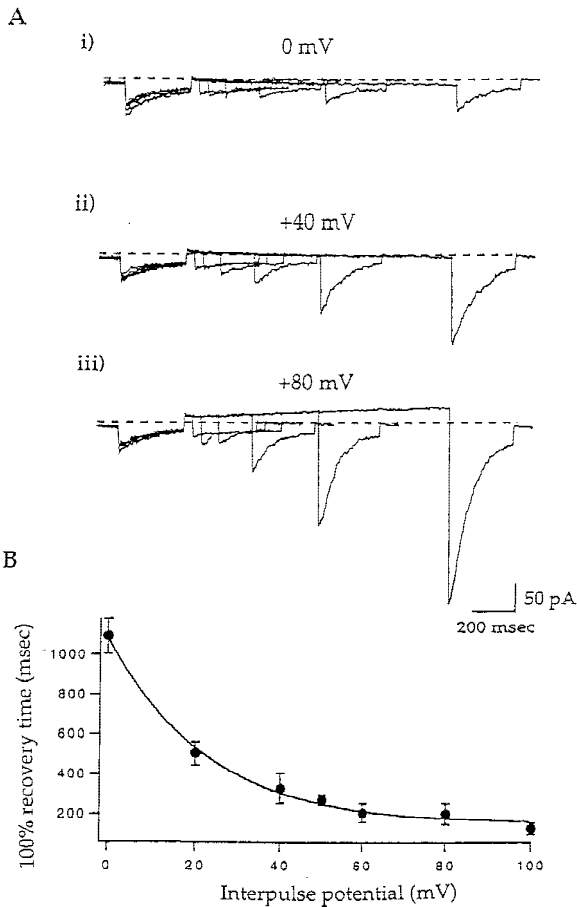


**Fig. 3.** Voltage- and time-dependent recovery of  $I_{\text{GINa}}$ . The holding potential was stepped from 0 to  $-100$  mV for 200 msec (first pulse). The cell was then clamped at one potential (interpulse potential) for different times, and then the holding potential was switched to  $-100$  mV again. The time increased in an exponential manner (20, 40, 80, 160, 320, 640, 1280 msec). The interpulse potentials were between 0 and  $+100$  mV. The recovery of  $I_{\text{GINa}}$  was both voltage- and time-dependent. *B* plots the time at which  $I_{\text{GINa}}$  had fully recovered to the level observed during the first hyperpolarizing pulse to  $-100$  mV against the interpulse potential. The curve could be fitted with a single mono-exponential function.

currents grow with time during pulses to positive potentials. Our previous experiments did not reveal such behavior (Parekh, 1996). However, in those experiments,  $\text{Cs}^+$  was the main intracellular cation in the patch pipette so that the  $\text{Na}^+$  reversal potential ( $E_{\text{Na}}$ ) was  $+70$  mV. Voltage pulses to positive potentials would therefore not be expected to generate much outward  $I_{\text{GINa}}$  because of the small electrical driving force. One possible way to measure outward currents through GINa channels would be to use symmetric  $\text{Na}^+$  solutions. Under these conditions,  $E_{\text{Na}}$  would be close to 0 mV and so large positive pulses should generate prominent outward currents that grow with time. In Fig. 4,  $I_{\text{GINa}}$  was recorded with 145 mM  $\text{Na}^+$  glutamate (instead of  $\text{Cs}^+$  glutamate) in the pi-

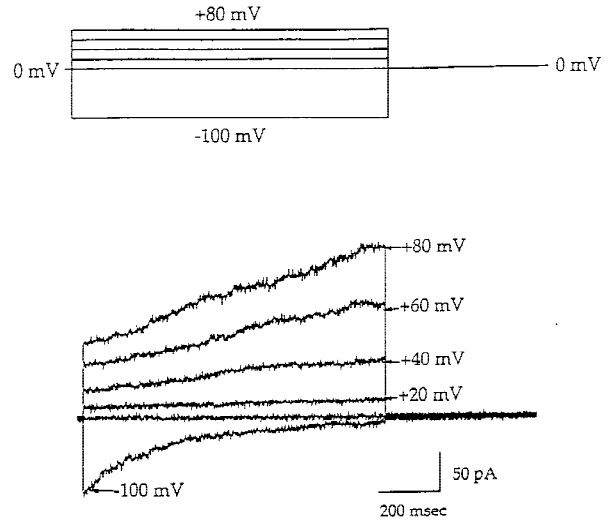


**Fig. 4.** Slow secondary outward currents in symmetrical  $\text{Na}^+$  solutions. With equal concentrations of  $\text{Na}^+$  in the patch pipette and bath solutions, a slowly developing secondary current is seen at positive potentials. Note that  $I_{\text{GINa}}$  still declines at  $-100$  mV. No inward currents are seen on pulsing back to 0 mV because this is now the reversal potential for  $I_{\text{GINa}}$  with symmetric  $\text{Na}^+$  solutions.

pette solution and 145 mM NaCl in the bath. Outward currents were observed positive to 0 mV. Pulses to positive potentials now generated a biphasic current. In addition to an instantaneous increase in outward current, a second phase was revealed which grew slowly with time. At  $+20$  mV this secondary component was small, but it became very prominent at potentials  $>+40$  mV (Fig. 4).

## Discussion

Unlike their counterparts in excitable cells,  $\text{Na}^+$ -selective channels in nonexcitable cells are not thought to exhibit any direct voltage-dependent behavior. Membrane voltage affects the current indirectly, only through changes in the electrical driving force. For the  $\text{Na}^+$  channels of renal epithelia, human A-431 cells and rat macrophages, channel activity was largely independent of membrane potential (range  $-100/-60$  to  $+30$  mV) even when patches were held at negative voltages over a time course of seconds (Negulyaev, Vedernikova & Mozhayeva, 1994; Negulyaev & Vedernikova, 1994; Palmer & Frindt, 1988). Only in one study on renal epithelial  $\text{Na}^+$  channels has voltage been shown to affect transitions between open and closed states, but this effect was thought to be modest at best (Hamilton & Eaton, 1985). This is all in marked contrast to the GTP-induced  $\text{Na}^+$ -selective current we now describe in RBL cells. We have found that this  $\text{Na}^+$  conductance is strongly voltage-dependent. Depolarizations substantially increase the conductance in both a voltage- and time-dependent man-



ner, whereas hyperpolarizations reduce it. This is particularly striking for two reasons. First, the  $\text{Na}^+$  current does not activate in the absence of GTP analogues. Depolarizations fail to elicit any  $\text{Na}^+$  current, demonstrating that it is not a pure voltage-operated  $\text{Na}^+$  channel. Second, the current develops at a fixed voltage (e.g.,  $-30$  mV) without any need to depolarize the membrane potential.

Three main mechanisms may be proposed to account for this behavior of GINa channels. One possibility is that the channels are voltage-gated  $\text{Na}^+$  channels in that depolarization increases open probability whereas hyperpolarization reduces it, but the channels cannot conduct  $\text{Na}^+$  ions unless some signal induced by  $\text{GTP}\gamma\text{S}$  is bound to the channel. Depolarization would result in an open but nonconducting state, which is alleviated by  $\text{GTP}\gamma\text{S}$ .

Another possibility is that the channel has no intrinsic voltage sensitivity, but instead the binding and unbinding of the activating signal is voltage-dependent. The final activating molecule is unlikely to be  $\text{GTP}\gamma\text{S}$  itself, but rather a product of a pathway activated by the GTP analogue (Parekh, 1996). Depolarization would increase binding of the signal whereas hyperpolarization would promote dissociation. Such voltage-dependent binding and unbinding would be similar to the regulation of N-type calcium channels by G proteins in peripheral neurons (Bean, 1989).

Finally, a third explanation for the voltage-dependent behavior is that the underlying mechanism is similar to that seen in HERG channels (Smith, Baukowitz & Yellen, 1996; Spector et al., 1996). HERG channels are voltage-gated  $\text{K}^+$  channels whose activation kinetics are slower than those that give rise to inactivation. At positive potentials, inactivation is faster than activation and this results in only small outward currents. On repolarization however, large inward tail currents are generated which decline as the channel deactivates. The slowly developing outward  $\text{Na}^+$  current at positive potentials (Fig. 4) would be consistent with this, since large depolarization accelerate activation of HERG. In this scenario,  $\text{GTP}\gamma\text{S}$  would be required for channel activity, but the mechanism that underlies the voltage-dependent behavior would be intrinsic to the channel protein itself.

Regardless of the specific mechanism, our results demonstrate that a nonvoltage-activated  $\text{Na}^+$  channel undergoes prominent voltage-dependent transitions in the presence of a cytoplasmic activating signal. Although  $I_{\text{GINa}}$  differs from voltage-dependent  $\text{Na}^+$  channels in terms of its selectivity, pharmacology and mechanism of activation, the finding that GINa channels are voltage-dependent suggests that there may be regions of similarity between these two types of channels as well.

Is  $I_{\text{GINa}}$  restricted to RBL cells? Steady-state  $I_{\text{GINa}}$  is very small at potentials more negative than  $-50$  mV, and

this is due to the marked voltage-dependent decrease in whole cell GINa conductance. Because the holding potential of most patch clamp experiments in nonexcitable cells is in the range of  $-80$  to  $-60$  mV, GINa channels would support very little  $\text{Na}^+$  current and therefore would be hard to detect at these potentials. It is conceivable that  $I_{\text{GINa}}$  is not restricted to RBL cells, but may be more widely distributed. Future experiments on other cell-types employing different holding potentials are required to address this.

What physiological role might  $I_{\text{GINa}}$  fulfill? We have been unable to activate the current through receptor stimulation (Parekh, 1996). Furthermore, as nonexcitable cells tend not to express voltage-activated channels, it is unclear why a  $\text{Na}^+$  channel should be expressed other than in  $\text{Na}^+$ -transporting cells, since the depolarization itself would not activate any other channels. It is striking however that  $I_{\text{GINa}}$  is very large (several hundred pA). The single-channel conductance appears low (Parekh, 1996), which would indicate several hundred functional copies of the channel within the plasma membrane. It seems unlikely that cells, even transformed ones, would make such large amounts of protein without a role in cell function.

I thank Professor Alison F. Brading and Drs. Leonardo Fierro and Heinz Terlau for comments on the manuscript. This work was supported by the Wellcome Trust. A.B.P. is the Sir E.P. Abraham Research Fellow at Keble College, Oxford.

## References

- Bean, B.P. 1989. Neurotransmitter inhibition of neuronal calcium currents by changes in channel voltage dependence. *Nature* **340**:153–156
- Garty, H., Benos, D.J. 1988. Characteristics and regulatory mechanisms of the amiloride-blockable  $\text{Na}^+$  channel. *Physiol. Rev.* **68**:309–373
- Hamill, O.P., Marty, A., Neher, E., Sakmann, B., Sigworth, F. 1981. Improved patch clamp techniques for high-resolution current recordings from cells and cell-free membrane patches. *Pfluegers Arch.* **391**:85–100
- Hamilton, K.L., Eaton, D.C. 1985. Single-channel recordings from amiloride-sensitive epithelial sodium channel. *Am. J. Physiol.* **249**:C200–207
- Hancox, J. C., Levi, A.J. 1995. Na–Ca exchange tail current indicates voltage dependence of the Cai transient in rabbit ventricular myocytes. *J. Cardiovasc. Electrophysiol.* **6**:455–470
- Harootunian, A.T., Kao, J.P., Eckert, B.K., and Tsien, R.Y. 1989. Fluorescence ratio imaging of cytosolic free  $\text{Na}^+$  in individual fibroblasts and lymphocytes. *J. Biol. Chem.* **264**:19458–19467
- Hille, B. 1992. Ionic channels of excitable membranes. 2nd edition Sinauer pp. 59–81. 348–351. Sunderland, MA
- Kameyama, M., Kakei, M., Sato, R., Shibusaki, T., Matsuda, H., Irisawa, H. 1984. Intracellular  $\text{Na}^+$  activates a  $\text{K}^+$  channel in mammalian cardiac cells. *Nature* **309**:354–356
- Kaplan, M.R., Mount, D.B., Delpire, E. 1996. Molecular mechanisms of  $\text{NaCl}$  cotransport. *Annu. Rev. Physiol.* **58**:649–668

- Motulsky, H.J., Insel, P.A. 1983. Influence of sodium on the alpha 2-adrenergic receptor system of human platelets. Role for intraplatelet sodium in receptor binding. *J. Biol. Chem.* **258**:3913–3919
- Negulyaev, Y.A., Vedernikova, E.A. 1994. Sodium-selective channels in membranes of rat macrophages. *J. Membrane Biol.* **138**:37–45
- Negulyaev, Y.A., Vedernikova, E.A., Mozhayeva, G.N. 1994. Several types of sodium-conducting channel in human carcinoma A-431 cells. *Biochimica et Biophysica Acta* **1194**:171–175
- Palmer, L.G. 1992. *Ann. Rev. Physiol.* **54**:51–66
- Palmer, L.G., Frindt, G. 1988. Conductance and gating of epithelial sodium channels from rat cortical collecting tubules. *J. Gen. Physiol.* **92**:121–138
- Parekh, A.B. 1996. Nonhydrolyzable analogues of GTP activate a new Na<sup>+</sup> current in a rat mast cell line. *J. Biol. Chem.* **271**:23161–23168
- Smith, P.L., Baukrowitz, T., Yellen, G. 1996. The inward rectification mechanism of the HERG cardiac potassium channel. *Nature* **379**:833–836
- Spector, P.S., Curran, M.E., Zou, A., Keating, M.T., Sanguinetti, M.C. 1996. Fast inactivation causes rectification of the I-Kr channel. *J. Gen. Physiol.* **107**:611–619